ACS Catalysis

pubs.acs.org/acscatalysis

Research Article

Supported Electrophilic Organoruthenium Catalyst for the Hydrosilylation of Olefins

Uddhav Kanbur,[#] Ryan J. Witzke,[#] Jiayi Xu, Magali S. Ferrandon, Timothy A. Goetjen, A. Jeremy Kropf, Frédéric A. Perras,* Cong Liu, T. Don Tilley,* David M. Kaphan,* and Massimiliano Delferro*

Cite This: *ACS Catal.* 2023, 13, 13383−13394

Read Online

ACCESS | Metrics & More | Article Recommendations | Supporting Information

ABSTRACT: A series of supported electrophilic organoruthenium complexes has been synthesized via surface organometallic chemistry (SOMC) techniques and applied to the selective hydrosilylation of olefins. The air-sensitive 16e$^-$ complex Cp*RuMes(PCy_3) (**1**) (Cp* = pentamethylcyclopentadienyl, Mes = mesityl) was synthesized by the treatment of Cp*RuCl(PCy_3) with mesityl Grignard MesMgBr. This species was chemisorbed onto sulfated zirconia SO_4/ZrO_2, but the resulting material was inactive toward cyclohexene hydrosilylation with phenylsilane. Instead, Cp*RuMes(PCy_3) was treated with phenylsilane ($PhSiH_3$) to provide a ruthenium disilyl hydride complex Cp*RuH(SiH_2Ph)$_2$(PCy_3) (**3**), which was fully characterized by NMR spectroscopy and single-crystal X-ray diffraction. Grafting this species onto SO_4/ZrO_2 resulted in the formation of phenylsilane along with the surface electrophilic species [Cp*RuH(R)(X-SiHPh)(PCy_3)] (R = H, O_3S−O or O_3Zr−O; **4a, 4b**, X = O_3S−O, and O_3Zr−O, respectively) as the major species. Material **4** was characterized via a combination of spectroscopic techniques including dynamic nuclear polarization (DNP)-enhanced solid-state NMR spectroscopy, diffuse reflectance infrared Fourier transform spectroscopy (DRIFTS), X-ray absorption spectroscopy (XAS), and density function theory (DFT) calculations. Capping the remaining acid sites on **4** with Me_3Si-$SiMe_3$ provides **5**, which significantly reduces side reactions, such as olefin isomerization and silane redistribution. Catalyst **5** is a highly robust and selective hydrosilylation catalyst and can be recycled up to 5 times without significant diminishment of activity. Exclusive anti-Markovnikov regiochemistry, cis-addition selectivity, and the inactivity of secondary and tertiary silanes provide support for the proposed Glaser−Tilley mechanism involving cationic ruthenium silylene species analogous to homogeneous systems.

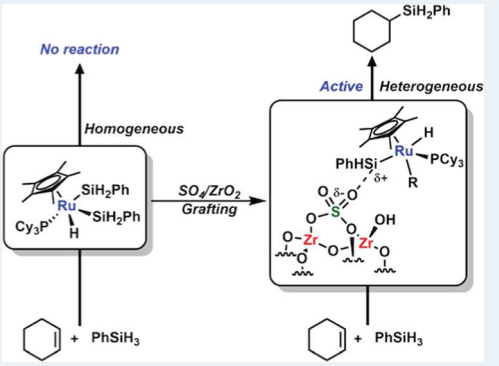

KEYWORDS: *hydrosilylation, surface organometallic chemistry, ruthenium, solid-state NMR, surface modification*

INTRODUCTION

Hydrofunctionalization, the addition of an E−H bond (E = C, Si, B, P, N, O, Sn) across an unsaturated bond, is an important chemical transformation used in industry to upgrade olefins and other feedstocks to value-added chemicals.[1] In particular, metal-catalyzed olefin hydrosilylation[2] finds widespread application in the commercial manufacture of silicone-based surfactants, fluids, molding products, release coatings, and pressure-sensitive adhesives.[3] Consequently, hydrosilylation has emerged as one of the largest-scale applications of homogeneous catalysis.[4] For more than three decades, precious metal compounds containing Pt, Pd, and Rh have been used almost exclusively as hydrosilylation catalysts. The hydrosilylation of alkenes catalyzed by these expensive transition-metal catalysts is often accompanied by side reactions such as alkene isomerization, oligomerization, polymerization, and hydrogenation as well as redistribution and dehydrogenation of the silanes and reactions in which both substrates take part.[5] Platinum compounds, such the Karstedt and Speier catalysts, are the most widely used industrial catalysts,[6−8] although they suffer from chemical limitations such as incompatibility with amino-substituted olefins, poor catalyst recovery, and a tendency to catalyze competing isomerization of terminal alkenes to the corresponding internal isomers.[9]

The most common hydrosilylation mechanisms, the Chalk−Harrod and modified Chalk−Harrod mechanisms (Scheme 1a), allow for olefin isomerization, the formation of Markovnikov and anti-Markovnikov products, and over-hydrosilylation resulting from product reentering the catalytic cycle (e.g., when primary or secondary silanes are used). An alternative cycle, the Glaser−Tilley mechanism, eliminates some of these undesirable pathways.[10−21] Depicted in Scheme 1b, this mechanism centers around a cationic Ru silylene

Received: July 25, 2023
Revised: September 18, 2023
Published: October 3, 2023

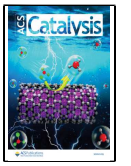

Scheme 1. (a) Metal-Catalyzed Hydrosilylation of Olefins via Chalk−Harrod or Modified Chalk−Harrod Mechanism; (b) [Ru═Si]$^+$ Catalyzed Hydrosilylation via Direct Addition of the Silylene Si−H Bond to an Olefin (Glaser−Tilley Mechanism)

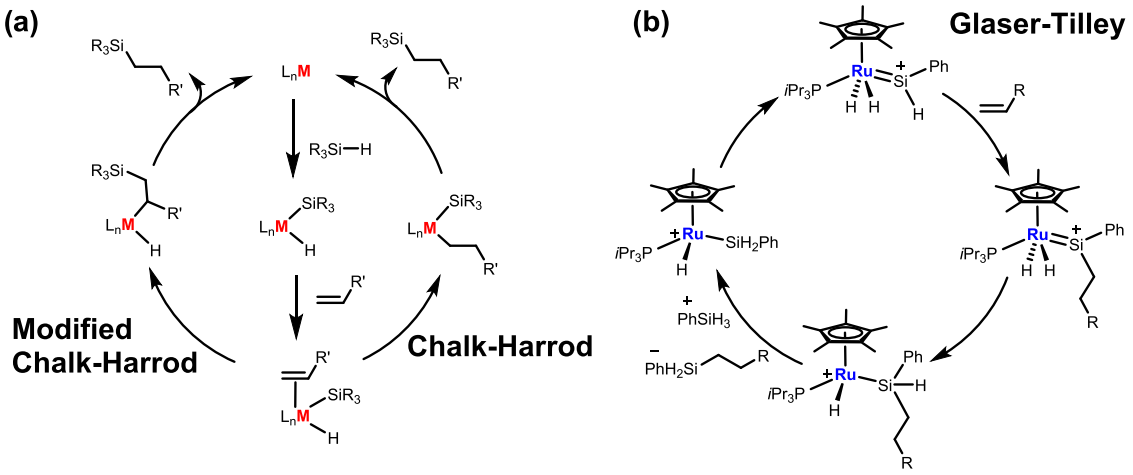

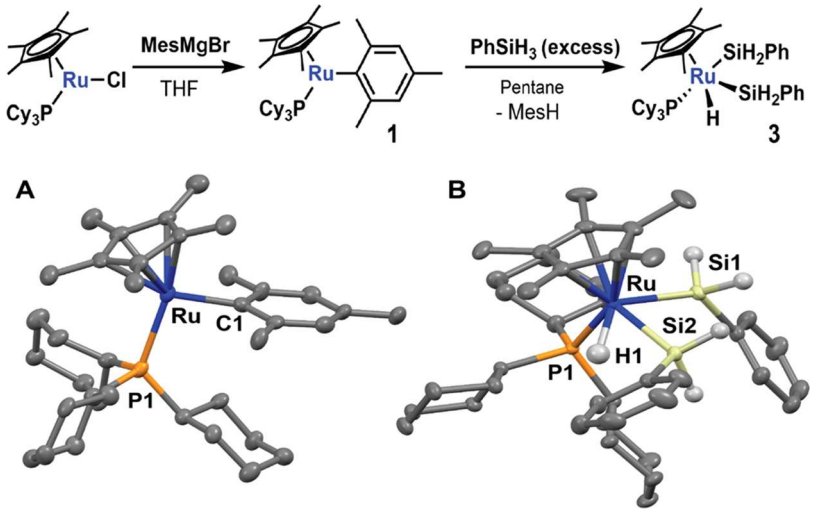

Figure 1. Top: Synthesis of organoruthenium 16e$^-$ complex **1** and organoruthenium 18e$^-$ complex **3**. Bottom: Crystal structures of (A) **1** (selected bond lengths: Ru−P1, 2.427 Å; Ru−C1, 2.100 Å), and (B) **3** (selected bond lengths: Ru−P1, 2.353 Å; Ru−H1, 1.584 Å; Ru−Si1, 2.401 Å; Ru−Si2, 2.419 Å). Thermal ellipsoids are set at the 50% probability level. All hydrogen atoms except those depicted are omitted for clarity.

complex.[22] The electrophilicity of Si bonded to Ru enables direct olefin insertion into the Si−H bond.

In the Glaser−Tilley mechanism, the silane product is eliminated through a series of 1,2 hydrogen migrations from Ru to Si. The silylene intermediate is then reformed via a double Si−H activation of a primary silane. This unique insertion pathway via nucleophilic attack of the olefin at the electrophilic Si atom enables the high selectivity of this mechanism. Only anti-Markovnikov products resulting from syn-insertion are observed. Inspired by these unique results, we envision that supporting Ru organometallic precursors on acidic supports, such as sulfated zirconia, will not only stabilize these catalysts toward decomposition[23,24] but also allow the formation of a cation-like Ru center on the surface,[25] which is needed to yield the metal-silylene active site (Scheme 1b). We have recently reported that the chemisorption of (^{dm}Phebox)-Ir(OAc)$_2$(OH$_2$) (^{dm}Phebox = 2,6-bis(4,4-dimethyloxazolinyl)-3,5-dimethylphenyl) on sulfated zirconia generates an electrophilic, cation-like iridium center capable of activating C−H bonds at lower temperature than the homogeneous counterpart.[15,26] The enhanced reactivity of highly electrophilic molecular species on acidic oxide surfaces represents a new interface between homogeneous and heterogeneous catalysis, with its own challenges and opportunities.[27−30] For example, Marks and co-workers have reported the formation of cationic group IV metal centers stabilized on sulfated zirconia for olefin polymerization and hydrogenations.[27,31−34] The catalytic activities of these reactive surface species can considerably exceed their homogeneous analogues in some cases, even with the weakest coordinating counteranions.[27,35] While there are several known platinum-based recyclable hydrosilylation systems,[36−41] there are only a handful of examples of supported ruthenium complexes for hydrosilylation applications reported in the literature.[42−44] Another drawback of ruthenium-based catalysts is their low activity. For example, [(CH$_3$CN)$_3$RuCp]PF$_6$ supported on carbon-coated mesoporous silica provided a catalyst for the hydrosilylation of 1-hexyne; however, the stability of the surface species resulting from η^6-arene coordination led to very low catalytic activity, and a maximum turnover number of 2 was observed.[42] More recently, a site-isolated ruthenium catalyst on zirconia was shown to be effective in the hydrosilylation of ethylene with

https://doi.org/10.1021/acscatal.3c03399
ACS Catal. 2023, 13, 13383−13394

Scheme 2. Grafting of 3 onto SO_4/ZrO_2 Leading to a Mixture of Surface Species 4 (4a and 4b)

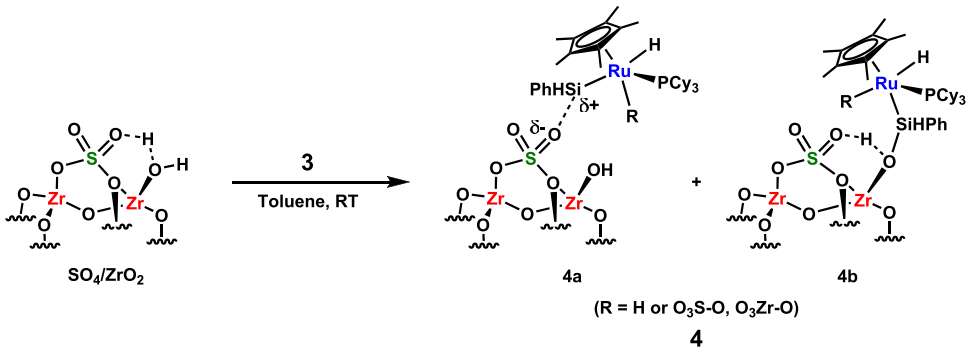

triethoxysilane.[44] The Ru/ZrO_2 catalyst was also recyclable, but a significant drop in yields was observed after three cycles. Hence, it is challenging to generate a robust surface-supported catalytically active ruthenium center. Herein, we describe a series of organoruthenium complexes amenable to surface organometallic chemistry, synthesized and chemisorbed on sulfated zirconia to promote the Glaser−Tilley olefin hydrosilylation mechanism in a heterogeneous system, thus making them separable from the reaction media and recyclable.

RESULTS AND DISCUSSION

Synthesis and Characterization of Molecular and Grafted Complexes. In order to generate a highly active and selective heterogenized hydrosilylation catalyst, an organometallic precursor to generate the electrophilic fragment upon grafting onto a highly acidic surface was needed. Complex $Cp^*RuCl(PCy_3)$[45] (Cy = cyclohexyl) reacted with mesitylmagnesium bromide in ether at −30 °C with an instantaneous color change from purple to deep blue to afford the coordinatively unsaturated, 16-electron complex $Cp^*RuMes(PCy_3)$ (**1**) in 60% yield after 18 h (Figure 1). The product was characterized by ^1H, ^{13}C, and ^{31}P NMR spectroscopy (Figures S14−S19). Note that the chemical shift at 37 ppm in the ^{31}P NMR spectrum is characteristic of organometallic ruthenium(II) phosphine complexes.[46] X-ray quality single crystals were grown from a concentrated pentane solution layered with hexamethyldisiloxane (HMDSO) and provided the structure shown in Figure 1.

The crystal structure of the two-legged piano stool complex revealed a $Ru-C_{Mes}$ bond length of 2.100(8) Å and a Ru−P length of 2.427(2) Å, consistent with the previously reported similar complex $Cp^*(^iPr_2MeP)RuCH_2Ph$.[47] Complex **1** was allowed to react with a suspension of sulfated zirconia[28] (SO_4/ZrO_2) in toluene at room temperature to afford the beige-colored $Cp^*RuMes(PCy_3)/SO_4/ZrO_2$ (**2**). The grafting reaction was also monitored by ^1H NMR spectroscopy, where the decrease of $Cp^*RuMes(PCy_3)$ signals was observed alongside the formation of free mesitylene and without the release of free tricyclohexyl phosphine. Inductively coupled plasma-atomic emission spectroscopy (ICP-AES) measurements of **2** revealed a 1 wt % Ru surface loading, consistent with the loading estimated from the consumption of **1** in an in situ ^1H NMR grafting experiment. In an initial experiment, phenylsilane, cyclohexene, and hexamethylbenzene as an internal standard and **2** in C_6D_6 were combined in an NMR tube at 70 °C and monitored at regular intervals by ^1H NMR spectroscopy. The formation of the desired product $Ph(Cy)SiH_2$ was not observed even after reaction for 96 h of reaction. However, $PhSiH_3$ disproportionation products were observed in appreciable quantities (43%). To understand the failure of **2** as an effective hydrosilylation catalyst, the material was studied by solid-state ^{13}C, ^{31}P, and ^1H NMR spectroscopy (Figures S29, S31, S28). The ^{31}P NMR spectrum of **2** featured three major species at 40, 23, and −10 ppm. To further understand the decomposition of the Ru fragment in **2**, PCy_3 and $O{=}PCy_3$ were exposed to sulfated zirconia to identify possible decomposition products in **2** by ^{31}P NMR spectroscopy (Figure S39a−d). PCy_3 on SO_4/ZrO_2 featured minor peaks at 71 and 40 ppm and a major peak at 23 ppm, assigned as the phosphine oxide, the protonated phosphonium, and the physisorbed phosphine, respectively, consistent with previous reports in the literature.[48,49] $O{=}PCy_3$ on SO_4/ZrO_2 featured a distribution of resonances centered at 72 ppm, attributed to different Lewis and Brønsted acid binding sites.[48,50] Based on the phosphine and phosphine oxide probe molecules, the ^{31}P spectrum of **2** showed the nearly complete release of PCy_3, with the peaks at 40 and 23 ppm attributed to the protonated phosphonium and physisorbed phosphine, respectively, with the unknown signal at −10 ppm being plausibly consistent with the upfield shift expected for dealkylated dicyclohexylphosphine. Thus, the inactivity of **2** is attributed to the instability of the resulting electrophilic, low-coordinate surface ruthenium species on sulfated zirconia. To obtain a stabilized surface complex, $Cp^*RuMes(PCy_3)$ (**1**) was allowed to react with phenylsilane in pentane, resulting in a change in color from blue to pale yellow along with the precipitation of a white solid. Isolation of this solid provided the analytically pure 18-electron complex $Cp^*RuH(SiH_2Ph)_2(PCy_3)$ (**3**) in 73% yield (Figure 1). The Ru−H resonance was observed as a doublet at −11.5 ppm ($J_{H,P}$ = 31 Hz) in the ^1H NMR spectrum, while the Si−H resonances were observed as two broad multiplets at 5.3 and 5.0 ppm. A singlet at 57 ppm was detected in the ^{31}P NMR spectrum.[51] A direct ^{29}Si signal was also identified at −0.37 ppm, similar to the silicon resonance at −1.1 ppm observed for the ruthenium silyl hydride complex $cis\text{-}(PMe_3)_4Ru(SiMe_2H)H$.[51] Single-crystal X-ray diffraction analysis revealed a spectroscopically consistent structure, as shown in Figure 1. The Ru−H distance of 1.584(5) Å in **3** is comparable to previously reported Ru−H distances in ruthenium(IV) silyl hydride complexes such as $(PMe_3)_3Ru(SiMe_3)H_3$, where Ru−H1 = 1.49(4), Ru−H2 = 1.64(5), and Ru−H3 = 1.43(4) Å in the latter complex.[51] The Ru−Si bond lengths (2.419(1) and 2.401(1) Å) and Ru−P (2.353(1) Å) in $Cp^*RuH(SiH_2Ph)_2(PCy_3)$ are also very similar to known values in the literature.[51]

https://doi.org/10.1021/acscatal.3c03399
ACS Catal. 2023, 13, 13383−13394

Scheme 3. Stoichiometric Reaction of the 3 with Anhydrous *p*-Toluenesulfonic Acid (PTSA)

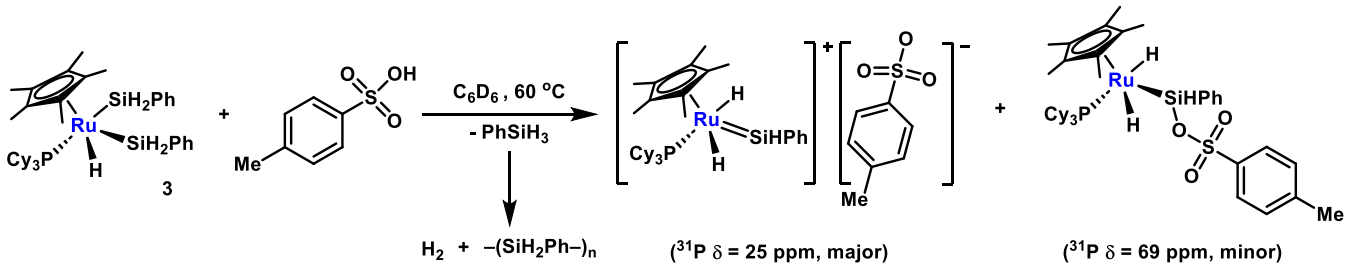

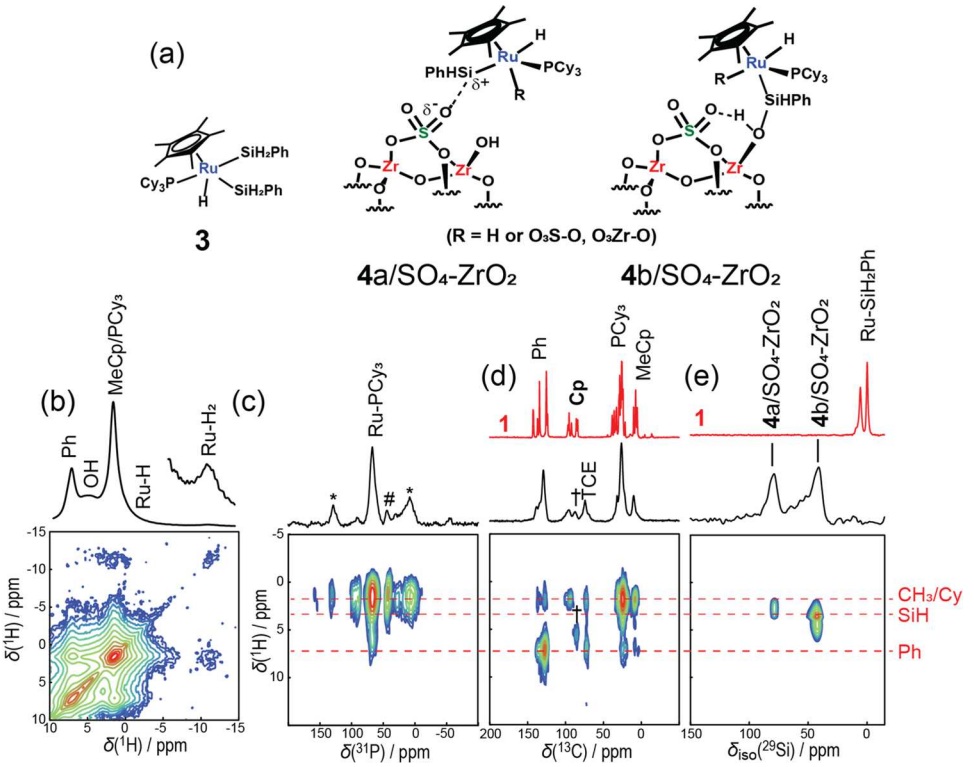

Figure 2. (a) Structures of the precursor **3** and the two species (**4a** and **4b**) formed upon grafting. (b) ^{1}H fast-MAS NMR spectrum (top) and ^{1}H 2D RFDR spectrum (bottom). (c) ^{31}P{^{1}H} CPMAS and 2D FSLG-HETCOR NMR spectra of **4**. (d) ^{13}C{^{1}H} CPMAS NMR spectrum of **3** (top, red) and DNP-enhanced CPMAS and 2D FSLG-HETCOR spectra of **4** (bottom). (e) ^{29}Si{^{1}H} CPMAS NMR spectrum of **3** (top, red) and DNP-enhanced CPMAS and 2D FSLG-HETCOR spectra of **4** (bottom). Dashed red lines are drawn along the ^{1}H dimension to highlight the different resolved ^{1}H species. Asterisks denote spinning sidebands; daggers denote the signals from an unknown impurity, and pound signs denote adsorbed PCy_3.

Complex $Cp^*RuH(SiH_2Ph)_2(PCy_3)$ (**3**) was also chemisorbed onto SO_4/ZrO_2 in toluene to provide the beige material **4** (Ru loading via ICP-AES = 0.6 wt %, Scheme 2), and an NMR scale grafting experiment revealed a decrease in the $Cp^*RuH(SiH_2Ph)_2(PCy_3)$ signals along with the formation of phenylsilane, hydrogen gas and signals consistent with polyphenylsilane (Figure S3). The initial formation of $PhSiH_3$ suggests protonolysis of the Ru−Si bond in **3**, while its subsequent consumption along with the growth of peaks corresponding to H_2 and $-(SiH_2Ph-)_n$ is consistent with a subsequent dehydrocoupling process.[51−53] The resulting material **4** exhibits a lower metal loading than **2** (0.6% wt. Ru, 0.44 Ru atoms/nm^2), but it is within the expected range for surface organometallic complexes formed via Lewis acid/base interactions with the SO_4/ZrO_2 surface (~0.1 mmol/g Brønsted acid sites and 0.29 mmol/g Lewis acid sites with a Brunauer−Emmett−Teller (BET) surface area of 186 m^2/g).[48,54] Note that no correlation was observed in the stoichiometric relationship between the acid sites and the grafted species, and both of these values indicate steric constraints during the grafting reaction. Note also that the ruthenium loadings are not affected significantly with an increase in the ruthenium concentration during the grafting reactions.

To further understand the nature of the grafting process onto sulfated zirconia, a stoichiometric reaction of the ruthenium precursor **3** with anhydrous p-toluenesulfonic acid (PTSA), in C_6D_6 at 60 °C was conducted and monitored by NMR spectroscopy (Scheme 3 and Figure S27).[55] Rapid evolution of gas was observed and was corroborated by the appearance of a signal at 4.47 ppm corresponding to H_2. In addition, new broad signals at 5−6 and 7−8 ppm were observed corresponding to poly(phenylsilane) species,[56] likely formed as a result of dehydrocoupling. The Ru−H doublet of $Cp^*RuH(SiH_2Ph)_2(PCy_3)$ at −11.5 ppm decreased in intensity, concomitant with the formation of a pair of doublets

https://doi.org/10.1021/acscatal.3c03399
ACS Catal. 2023, 13, 13383−13394

at −11.6 and −11.8 ppm integrating to two protons (Ru−H) and a new singlet at 1.6 ppm integrating to 15 protons (Cy). The Si−H signals of **3** at 5.26 and 4.97 ppm are completely consumed, and no new signals appear in that characteristic region. A new multiplet observed at 8.18 ppm was assigned to a silylene Ru = Si(*H*)Ph proton, previously reported at 8.15 ppm for $[Cp^*(^iPr_3P)RuH_2(=SiHMes)][CB_{11}H_6Br_6]$ by Tilley and co-workers.[12] Analysis of the ^{31}P NMR spectrum revealed consumption of the parent signal at 57 ppm, which is replaced by a major peak at 25 ppm and a small signal at 69 ppm (Figure S28). The latter signal is also observed in the solid-state NMR analysis (Figure 2) of **4**, indicating that a similar species is formed on the SO_4/ZrO_2 surface. An analogous compound $Cp^*(P^iPr_3)Ru(H)_2(SiHPhOTf)$[57] was previously reported and has a ^{31}P chemical shift of 79 ppm. Thus, the reaction of **3** with PTSA results in a mixture of species, the major species is consistent with $[Cp^*RuH_2(=SiHPh)(PCy_3)]$-[PTSA] ($\delta$ ^{31}P = 25 ppm) and a minor species consistent with Cp^*RuH_2(PTSA-SiHPh)(PCy_3) ($\delta^{31}P$ = 69 ppm). However, attempts to isolate these compounds failed, and intractable decomposition products were observed by NMR spectroscopy. Importantly, these in situ ruthenium-containing products were inactive for olefin hydrosilylation under the reaction conditions (vide infra).

Spectroscopic Characterization of Surface Species. The supported organoruthenium species **4** was characterized using a combination of spectroscopic techniques to elucidate the nature of the precatalyst. Diffuse reflectance infrared Fourier transform spectroscopy (DRIFTS) of **4** revealed distinct aliphatic (2900−3000 cm^{-1}) and aromatic (3100 cm^{-1}) C−H stretches that correspond to the ligands bound on ruthenium (Figure S29). A weak feature, observed at 1975 cm^{-1} was tentatively attributed to the Ru−H stretching frequency, similar to molecular ruthenium(IV) complexes containing a hydride and a silylene ligand[47] as well as surface-supported ruthenium hydrides such as $[(\equiv SiO)RuH(dmpe)_2]$.[58,59] Material **4** was also characterized by using an array of solid-state NMR experiments (Figure 2). The ^1H fast-MAS NMR spectrum of the species displayed clear resonances from the phenyl, aliphatic, and surface hydroxyl sites. In addition, a resonance at −11 ppm indicated the presence of a Ru hydride.[60] A through-space $^1H-^1H$ 2D correlation experiment (Figure 2b) showed clear cross-peaks between the aliphatic signals and both the phenyl and the hydride signals, confirming that all three species are in fact a part of the same complex. The ^{31}P NMR spectrum featured resonances centered at 70 ppm from Ru-PCy_3 species, similar to the molecular complex $[Cp^*(^iPr_3P)RuH_2(=SiHMes)]$-$[CB_{11}H_6Br_6]$ reported by Tilley et al. at δ = 65 ppm,[12] in addition to a weak resonance from adsorbed phosphine (Figure 2c).

A DNP-enhanced[61−63] ^{13}C CPMAS NMR spectrum was obtained for the grafted species, which was similar to that from the molecular precursor (Figure 2d). Two resonances were observed in the range expected for Cp* (95 and 86 ppm); however, the lower frequency site was not found to correlate with the Cp* methyl ^1H resonance in a $^{13}C\{^1H\}$ HETCOR spectrum, suggesting that it is instead from a supported species that is external to the complex, such as an alkoxy species. The higher frequency resonance agreed with the shift observed in the precursor in solution and suggested a rapid rotation of the Cp* group. This rotation was not seen in the crystalline precursor, presumably due to steric constraints or crystal packing effects. The HETCOR spectrum otherwise showed all of the expected short-range correlations, such as between aromatic protons and carbons and between aliphatic protons and carbons.

The DNP-enhanced $^{29}Si\{^1H\}$ CPMAS NMR spectrum of the grafted species was very different from that of the precursor (Figure 2e). The precursor featured two chemically inequivalent Ru-SiH_2Ph silyl species (δ ^{29}Si = −0.2 and 5.7 ppm), while the grafted species featured signals from two oxygen-bound silyl species generated from a reaction with the sulfated zirconia surface (δ ^{29}Si = 41 and 79 ppm). No signals were detected around 300 ppm from a silylene moiety, and other signals from −25 to −100 ppm indicated the formation of polysilanes upon grafting.[64−66] While the solid-state ^{29}Si NMR is not quantitative, it does suggest that the poly(phenylsilane) is generated from phenylsilane formed during the grafting reaction of **3** on SO_4/ZrO_2. Conley et al. have reported a reactive silylium species on sulfated zirconia of the type $[R_3Si][SO_4/ZrO_2]$, and the ^{29}Si CPMAS NMR spectrum revealed a major peak at 53 ppm assigned to the more electron-deficient R_3Si-O_x species.[67] The observed ^{29}Si chemical shifts of **4** are consistent with a similar silicon environment with a weakly coordinating sulfated zirconia surface. Such a structure {Ru−Si(H)(Ph)-OSO_3} can convert to a cationic ruthenium silylium species $[Ru{=}SiHPh][OSO_3]$ under catalytic conditions, similar to the proposed active species of the Glaser−Tilley hydrosilylation mechanism.

DFT calculations of the ^1H, ^{31}P, and ^{29}Si chemical shifts (Table S1) were performed to aid in the assignment of the spectra. In total, ten different structures were modeled (Table S1). All predicted Ru-SiH_2Ph ^{29}Si chemical shifts were close to those observed in the precursor, while most Ru-SiH(O)Ph species fell close to those from the two species observed experimentally. Of these remaining structures, only the dihydride species reproduced the observed hydride ^1H chemical shift of −11 ppm, with ZrO- and SO-bound silanes having DFT-calculated ^{29}Si shifts of 29.0 and 62.2 ppm, which would agree with those observed experimentally (Figure S38). Monohydrides are predicted to resonate around −5.2 and −3.4 ppm, which is not observed experimentally; however, this may be caused by a lack of resolution at higher frequencies due to overlap from the aliphatic signals (see Figure S36). The ^{29}Si signals could also be assigned to analogous hydride-free species.

X-ray absorption spectroscopy (XAS) at the Ru K edge was used to further investigate the structure of **4** (Figure 3a). Based on the greater white line intensity of **4** compared to **3**, X-ray absorption near-edge structure (XANES) indicates an increase in oxygen donors in the inner coordination sphere of Ru, suggesting the possibility of at least some proteolytic substitution at the metal center in addition to the S atom (Scheme 2). The extended X-ray absorption fine structure (EXAFS, Figure 3b) qualitatively indicates that the average Ru nearest neighbor bond length in **4** has decreased relative to the molecular precursor (based on the increased oscillation period), while either increased disorder to the Ru environment or destructive interference between scattering paths accounts for the lower amplitude at high k. This is consistent with structure **4***a*/**4b** as a major species on SO_4/ZrO_2, in which a longer Ru−Si bond is replaced with a shorter Ru−O bond, also in agreement with SS NMR (vide supra).

Model-dependent quantitative EXAFS fits are possible using the measured crystal structure of **3** (Table 1). The

https://doi.org/10.1021/acscatal.3c03399
ACS Catal. 2023, 13, 13383−13394

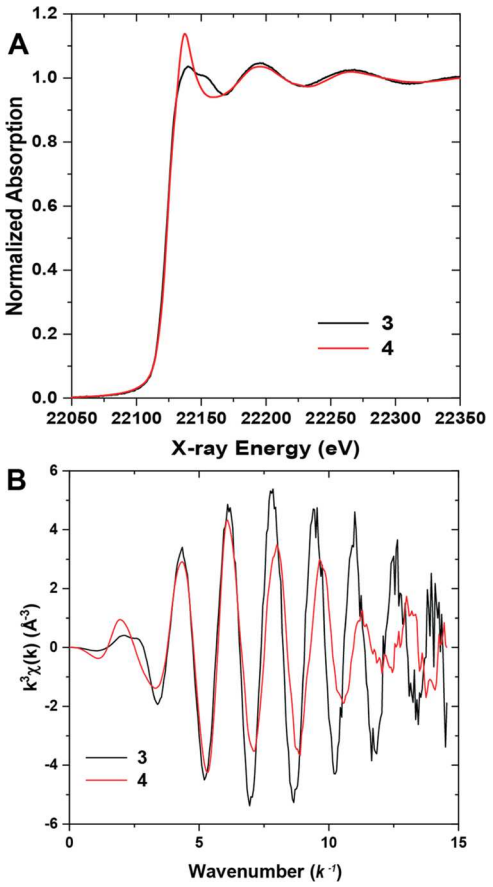

Figure 3. (A) Ru K edge XANES and (B) k^3 $\chi(k)$ EXAFS for organoruthenium complex **3** and supported material **4**.

coordination numbers have been assumed to be correct, while all of the nearest neighbor (NN) C atoms in Cp* are described by a single distance shift and σ^2. Similarly, Si and P are all described by a single distance shift relative to the crystal structure and σ^2. The fit mismatch is only 0.8%, which indicates a good match to the model, although the bond length shifts are somewhat large at ±0.04 Å. For **4**, a Ru−O bond has been substituted for a Ru−Si bond. The fit results confirm the average NN bond length decrease from **3** to **4** and demonstrate that the model is consistent with the spectra. The amplitude reduction factor has been fixed to the value determined from a Ru metal foil. Without this concession, the correlations between fit parameters are very high. The results when fitting S_0^2 are given in Table S2.

The structure of ruthenium species on the surface based on consolidated spectroscopic results is likely of the type [Cp*RuH(R)(X-SiHPh)(PCy_3)] (R = H, O_3S−O or O_3Zr−O; **4a, 4b**, X = O_3S−O, O_3Zr−O, respectively, Scheme 2), which is a mixture of ruthenium monohydrides and dihydrides. Species of type **4a** containing a weak Ru−Si(H)(Ph)−O−SO_3 linkage possibly reversibly converted to the mechanistically relevant cationic species [Ru═SiHPh][O−SO_3] under catalytic conditions, analogous to the molecular species formed during the reaction of **3** with PTSA.

Catalytic Hydrosilylation of Olefins. In an NMR scale experiment, cyclohexene and $PhSiH_3$ were converted to $Ph(Cy)SiH_2$ in the presence of catalyst **4** (1 mol % Ru) in C_6D_6 at 70 °C in 88% yield after 72 h, corresponding to 88 turnovers in this period (Table 2, Entry 4; for solvent effect see

Table 2. Catalyst Efficacy and Recycling Data for the Hydrosilylation of Cyclohexene with Phenylsilane[a]

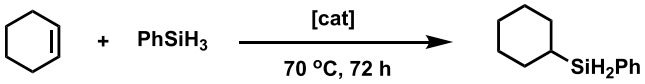

entry	catalyst	yield[b]
1	Cp*RuMes(PCy_3) (**1**)	<1
2	**2**	<1
3	Cp*RuH(SiH_2Ph)$_2$ (PCy_3) (**3**)	<1
4	**4**	88, 83[c], 61[d], 13[e]
5	**5**[i]	92, 89[c], 91[d], 88[e], 88[f], 54[g], 21[h]

[a]Conditions: benzene-d_6, [cyclohexene]/[PhSiH3] = 1:1, 1 mol % Ru, 70 °C, 96 h [b]NMR yield [c]1st round of catalyst recycling [d]2nd round of catalyst recycling [e]3rd round of catalyst recycling [f]4th round of catalyst recycling [g]5th round of catalyst recycling [h]6th round of catalyst recycling [i]72 h reaction time

Table S2). To rule out leaching of chemisorbed ruthenium species into the solution during catalysis, a partially converted reaction mixture of **4**, cyclohexene, and phenylsilane (18 h, 39% $Ph(Cy)SiH_2$ yield) was filtered to separate **4** and was allowed to further react at 70 °C. No further conversion of starting materials was observed, supporting the absence of catalytically active homogeneous species in the system. Additionally, the molecular complex Cp*RuH-(SiH_2Ph)$_2$(PCy_3) (**3**) was inactive toward cyclohexene hydrosilylation, and no conversion of the reactants was seen after 72 h at 70 °C (Table 2, Entry 3). A control experiment was also conducted with $PhSiH_3$, cyclohexene, and unmetalated SO_4/ZrO_2 under the same reaction conditions. The reaction only produced the silane redistribution species, Ph_2SiH_2, Ph_3SiH, and SiH_4; no change in the reaction composition was observed

Table 1. Ru K Edge EXAFS Fit Results after Setting S_0^2 (Simultaneous k^n Weighting, n = 1, 2, 3) and S_0^2 = 0.68(7) from Ru Foil

sample	k range ($Å^{-1}$)/R range (Å)	path	N	S_0^2	ΔR (Å) (vs xrd of 2)	R (Å)	σ^2 ($\times10^{-3}$ $Å^2$)	ΔE_0 (eV)	R-factor (%)
3	3.3−14.2/1.0−2.6	Ru−C_1	3	0.68	−0.042 ± 0.010	2.220	0.4 ± 0.7	1.9 ± 1.3	0.8
		Ru−C_2	2		−0.042 ± 0.010	2.262	0.4 ± 0.7		
		Ru−P	1		0.045 ± 0.009	2.397	1.3 ± 0.6		
		Ru−$Si_{1,2}$	2		0.045 ± 0.009	2.454	1.3 ± 0.6		
4	3.5−14.2/1.0−2.4	Ru−O	1	0.68		2.11 ± 0.06	2.0 (set)	2.2 ± 1.8	0.9
		Ru−C_1	3		−0.061 ± 0.011	2.200	1.3 ± 1.7		
		Ru−C_2	2		−0.061 ± 0.011	2.241	1.3 ± 1.7		
		Ru−P	1		0.051 ± 0.019	3.404	6.1 ± 2.1		
		Ru−Si	1		0.051 ± 0.019	2.461	6.1 ± 2.1		

https://doi.org/10.1021/acscatal.3c03399
ACS Catal. 2023, 13, 13383−13394

Table 3. Olefin and Silane Scope for Hydrosilylation[a]

Entry	Catalyst	Olefin	Silane	Product	Time (h)	Yield[a]
1	4		$PhSiH_3$	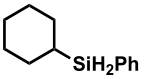	96	88[b]
2	4		$PhSiH_3$	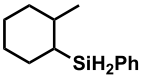	72	78[b,d]
3	4	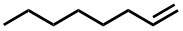	$PhSiH_3$	silane redistribution	72	< 1[c]
4	4		Ph_2SiH_2	silane redistribution	48	< 1[b,c]
5	4		$PhMe_2SiH$	silane redistribution	48	< 1[b,c]
6	5	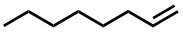	$PhSiH_3$		48	80[e]
7	5		$PhSiH_3$	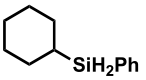	72	92

[a]Conditions: benzene-d_6, [olefin]/[silane] = 1:1, 1 mol % Ru, 70 °C [b]NMR yield [c]Silane redistribution observed [d]Olefin isomerization observed [e](±)*trans*-1-$PhSiH_2$-2-Me-cyclohexane

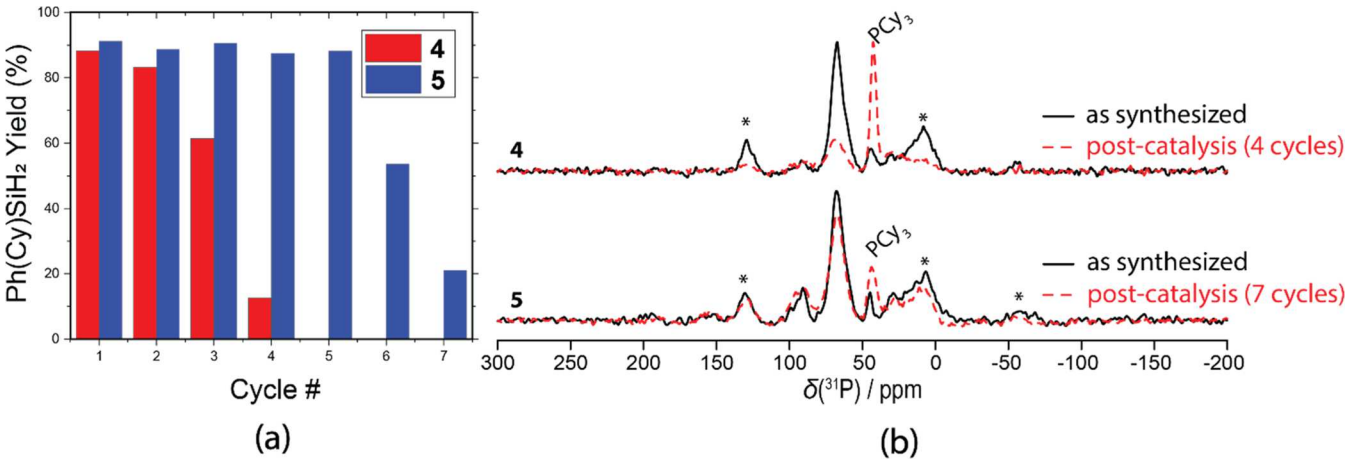

Figure 4. (a) Recyclability of catalysts **4** and **5** for the hydrosilylation of cyclohexene with phenylsilane and (b) ^{31}P CPMAS NMR spectra acquired for samples **4** and **5** both in their as-synthesized forms (black) in addition to after 4 and 7 catalytic cycles for **4** and **5**, respectively (red, dashed).

after 24 h of reaction, and no hydrogen was detected throughout the course of the reaction.[51,68] This also suggests that the expected protonolysis of the Si−H moiety in $PhSiH_3$ by surface hydroxyl groups in SO_4/ZrO_2 is unfavorable, and the silane redistribution is likely proton-catalyzed. Analogously, phenylsilane was allowed to react with **4** in the absence of cyclohexene and the results were monitored by ^1H NMR spectroscopy (Figure S10). The reaction proceeds with a mild effervescence of H_2 gas along with the appearance of polyphenylsilane resonances at 5.4−6.0 ppm and the silane disproportionation products, indicating a ruthenium-catalyzed silane dehydrocoupling reaction.[69,70] Catalyst **4**, exposed to air for 1 h, was also tested for the hydrosilylation of cyclohexene with phenylsilane. The reaction, conducted at 70 °C and monitored periodically by ^1H NMR spectroscopy, resulted in an only 5% yield of the desired $Ph(Cy)SiH_2$ product after 96 h. This indicates the loss of active sites during the air exposure process of **4** and that the deactivation appears to be irreversible.

No catalysis was observed with secondary and tertiary silanes such as Ph_2SiH_2 and $PhMe_2SiH$, respectively, consistent with prior observations in the $[Cp^*(^iPr_3P)(H)_2\text{-}Ru{=}Si(H)Ph{\cdot}Et_2O][B(C_6F_5)_4]$ system employed by Tilley and co-workers, wherein cationic ruthenium silylene species that contain at least one Si−H bond were necessary for catalysis and selectively transformed primary silanes.[10] To further investigate whether hydrosilylation with **4** follows a similar silylene-driven mechanism, 1-methylcyclohexene was reacted with $PhSiH_3$ at 70 °C for 72 h (Table 3). Analysis by NMR spectroscopy indicated the formation of (±)*trans*-1-$PhSiH_2$-2-Me-cyclohexane in 78% yield, and the anti-Markovnikov regioselectivity via *cis*-addition is consistent with the proposed mechanism (Figure S5). The reaction of 1-octene with phenylsilane in the presence of **4** led to the formation of

https://doi.org/10.1021/acscatal.3c03399
ACS Catal. 2023, 13, 13383−13394

Scheme 4. Capping of Sulfated Zirconia Surface Acid Sites in 4 with Hexamethyldisilane to Provide $SiMe_3$-Capped 5

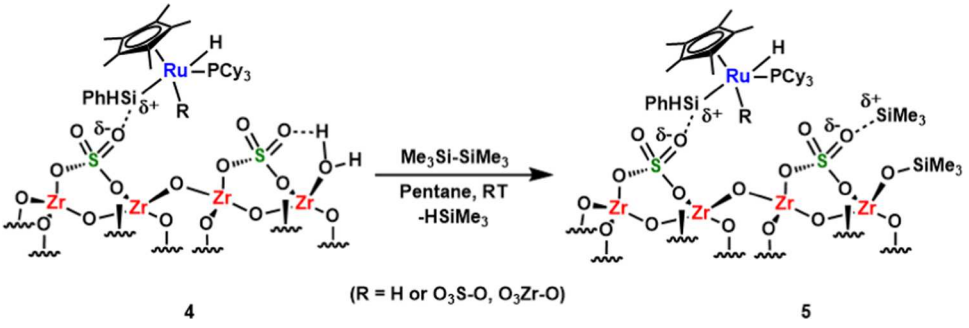

internal isomers of octene, along with silane redistribution; however, no hydrosilylated product was observed.

To test the recyclability of **4** in the hydrosilylation of cyclohexene with phenylsilane, the catalyst was isolated after the reaction and resubjected to the reaction conditions several times (Table 1). Hydrosilylation was initially performed at 70 °C for 96 h in deuterated benzene, and the catalyst was separated by filtration, washed thoroughly with benzene-d_6, and dried for 6 h under vacuum. The dry catalyst was used for the next run with fresh cyclohexene and phenylsilane and similarly monitored over 96 h. This process was repeated for four cycles, and the results are shown in Figure 4. Catalyst **4** demonstrates reasonable recyclability over three cycles with the yields of $Ph(Cy)SiH_2$ decreasing from 88 to 61%. The catalytic activity significantly diminished after the third cycle (13% yield).

It was hypothesized that capping of residual Brønsted acid sites might improve the catalyst performance by suppressing undesired background reactions such as silane redistribution, dehydrocoupling, and olefin isomerization and polymerization. To test this hypothesis, acid sites in **4** were capped with -$SiMe_3$ groups via addition of hexamethyldisilane (Scheme 4), affording catalyst **5**. Solid-state NMR analysis of this material revealed signals corresponding to the same hydride, phosphine, and silane species, suggesting that the structure of the ruthenium complex is preserved (Figures S28–S31). Additionally, the ^{29}Si NMR spectrum showed a new signal centered at 15 ppm, assigned to the O-TMS groups, formed as a result of capping the surface OH groups. Phenylsilane was allowed to react with **5** at 70 °C for 96 h, and this was monitored by ^{1}H NMR spectroscopy. Only trace amounts (<2%) of Ph_2SiH_2 were detected after 96 h with most of the $PhSiH_3$ remaining unconverted, indicating that phenylsilane is stable toward the sulfated zirconia support under reaction conditions. The reaction of cyclohexene with phenylsilane mediated by **5** at 70 °C provides the hydrosilylated product in 91% yield after 48 h. For comparison purposes, the hydrosilylation of cyclohexene with phenylsilane was performed with catalyst **5** and the homogeneous silylene complex $[Cp^*(^iPr_3P)RuH_2(=SiH\text{-}Mes)]^+[CB_{11}H_6Br_6]^-$ (1 mol % Ru) for 1 h at 80 °C.[12] Under these conditions, the TOF of catalyst **5** is lower (TOF = 8 in toluene and 11 in $CDCl_3$) than that of the homogeneous analogues (TOF = 79 in C_6H_5Br).[12] The difference in activity of **5** could be ascribed to multiple factors, including thermal stability at 80 °C (e.g., TOF = 20 in toluene at 70 °C), steric congestion of the support around the grafted organoruthenium fragment,[27] and stronger ion-pairing[25] of [Ru][SO_4/ZrO_2] related to [Ru] $[CB_{11}H_6Br_6]$, both of which limit the coordination of the substrate and reagent at the Ru center, thereby depressing the activity observed in homogeneous systems. In a separate control experiment, sulfated zirconia was treated with hexamethyldisilane, and the resulting material was tested for hydrosilylation of cyclohexene with phenylsilane under the same reaction conditions, resulting in no hydrosilylation and only traces of Ph_2SiH_2 detected from silane disproportionation (5% yield, Figure S13). In addition to suppressing undesirable side reactions, residual acid site capping was found to dramatically increase the longevity of the catalyst. Catalyst **5** is recyclable for 5 cycles without any loss in its activity, as shown in Figure 4, while in subsequent cycles, the catalyst has deactivated sufficiently to prevent reaching complete conversion. Note that each recycle step with **5** was monitored for a constant period of time (72 h) to reach full conversion, instead of at recommended lower conversions (less than 50%),[71] to observe the effects of passivation of the surface acid sites. Under these conditions, catalyst **5** is more stable than catalyst **4** toward deactivation, likely due to the lesser extent of side reactions, such as silane dehydrocoupling and disproportionation. Post-catalysis ^{1}H and ^{31}P solid-state NMR experiments were performed on both catalysts and revealed significant decomposition in **4**, as observed through the release of PCy_3 as the protonated phosphonium, while this decomposition pathway was suppressed in **5** (see Figure 4b). To further demonstrate the benefit of residual Brønsted acid site passivation, the reactions of 1-octene and phenylsilane at 70 °C in the presence of **5** were followed over 48 h. This resulted in the conversion of 1-octene to (1-octyl)phenylsilane in 80% yield, and internal isomers of 1-octene were observed in 20% yield along with the unconverted phenylsilane (Table 3, Entry 6). In contrast, the use of catalyst **4** in this reaction resulted exclusively in olefin isomerization and silane redistribution as mentioned above (Figures S7–S9). Thus, olefin isomerization of terminal alkenes was significantly reduced by capping acid sites, thereby allowing access to hydrosilylated products in good yields.

Consolidating the experimental catalytic results, a ruthenium-silylene-based mechanism, initially proposed by Glaser and Tilley (Scheme 1b), can be inferred for this heterogeneous system. The weakly coordinating nature of the sulfate group on the surface likely results in electrophilic ruthenium species **4a**, which can lead to the formation of a Ru(VI) moiety $[(H)Ru{=}SiHPh]^+$ under reaction conditions and is plausibly the resting state of the catalyst. The generation of cationic $[H{-}Ru{=}SiHPh]^+$ is necessary to facilitate catalysis based on the proposed catalytic cycle, and the lack of reactivity of secondary and tertiary silanes strengthens this hypothesis.

https://doi.org/10.1021/acscatal.3c03399
ACS Catal. 2023, 13, 13383–13394

CONCLUSIONS

In summary, the new organoruthenium complexes Cp*RuMes-(PCy_3) (**1**) and Cp*RuH(SiH_2Ph)$_2$(PCy_3) (**2**) were synthesized and immobilized onto an acidic sulfated zirconia support. X-ray and DFT studies suggested that the grafting process leading to the formation of **4** involves protonolysis of the Ru−Si bond instead of the Ru−H bond in Cp*RuH-(SiH_2Ph)$_2$(PCy_3). Passivation of acid sites in **4** led to the discovery of the more robust catalyst **5**, enabling access to the selective hydrosilylation of terminal olefins while suppressing olefin isomerization and silane redistribution pathways. **5** is a selective, scalable, and recyclable heterogeneous hydrosilylation catalyst, exclusively converting olefins to anti-Markovnikov products with primary silanes via the silylene mechanism.

ASSOCIATED CONTENT

Supporting Information

The Supporting Information is available free of charge at https://pubs.acs.org/doi/10.1021/acscatal.3c03399.

General discussion of synthetic and experimental procedures, instrumentation, and characterization of materials (PDF)

Optimized Structure (ZIP)

XYZ coordinate files for computational assessment of supported organoruthenium hydrosilylation catalyst to support mechanistic scenario (ZIP)

Accession Codes

CCDC 2234332−2234333 contain the supplementary crystallographic data for this paper. These data can be obtained free of charge via www.ccdc.cam.ac.uk/data_request/cif, or by emailing data_request@ccdc.cam.ac.uk, or by contacting The Cambridge Crystallographic Data Center, 12 Union Road, Cambridge CB2 1EZ, UK; fax: + 44 1223 336033.

AUTHOR INFORMATION

Corresponding Authors

Frédéric A. Perras − *Chemical and Biological Sciences Division, Ames National Laboratory, Ames, Iowa 50011, United States;* orcid.org/0000-0002-2662-5119; Email: fperras@ameslab.gov

T. Don Tilley − *Department of Chemistry, University of California, Berkeley, Berkeley, California 94720, United States; Chemical Sciences Division, Lawrence Berkeley National Laboratory, Berkeley, California 94720, United States;* orcid.org/0000-0002-6671-9099; Email: tdtilley@berkeley.edu

David M. Kaphan − *Chemical Sciences and Engineering Division, Argonne National Laboratory, Lemont, Illinois 60439, United States;* orcid.org/0000-0001-5293-7784; Email: kaphand@anl.gov

Massimiliano Delferro − *Chemical Sciences and Engineering Division, Argonne National Laboratory, Lemont, Illinois 60439, United States;* orcid.org/0000-0002-4443-165X; Email: delferro@anl.gov

Authors

Uddhav Kanbur − *Chemical Sciences and Engineering Division, Argonne National Laboratory, Lemont, Illinois 60439, United States*

Ryan J. Witzke − *Chemical Sciences and Engineering Division, Argonne National Laboratory, Lemont, Illinois 60439, United States*

Jiayi Xu − *Chemical Sciences and Engineering Division, Argonne National Laboratory, Lemont, Illinois 60439, United States;* orcid.org/0000-0003-1763-6251

Magali S. Ferrandon − *Chemical Sciences and Engineering Division, Argonne National Laboratory, Lemont, Illinois 60439, United States*

Timothy A. Goetjen − *Chemical Sciences and Engineering Division, Argonne National Laboratory, Lemont, Illinois 60439, United States; Department of Chemistry, Northwestern University, Evanston, Illinois 60208, United States;* orcid.org/0000-0001-8023-9107

A. Jeremy Kropf − *Chemical Sciences and Engineering Division, Argonne National Laboratory, Lemont, Illinois 60439, United States*

Cong Liu − *Chemical Sciences and Engineering Division, Argonne National Laboratory, Lemont, Illinois 60439, United States;* orcid.org/0000-0002-2145-5034

Complete contact information is available at: https://pubs.acs.org/10.1021/acscatal.3c03399

Author Contributions

#U.K. and R.J.W. contributed equally. The manuscript was written through contributions of all authors. All authors have given approval to the final version of the manuscript.

Funding

Work at Argonne National Laboratory was supported by the U.S. Department of Energy (DOE), Office of Basic Energy Sciences, Division of Chemical Sciences, Geosciences, and Biosciences, Catalysis Science Program under contract No. DE-AC-02−06CH11357. J.X. and C.L. would like to thank Laboratory Computing Resource Center (LCRC) at Argonne National Lab and National Energy Research Scientific Computing Center (NERSC) under contract number No. DE-AC02-05CH11231 with award number BES-ERCAP0023511. Use of the Advanced Photon Source is supported by the U.S. Department of Energy, Office of Science, and Office of the Basic Energy Sciences, under Contract No. DE-AC02-06CH11357. MRCAT operations at Sector 10 are supported by the Department of Energy and the MRCAT member institutions. ChemMatCARS operations at Sector 15 are supported by the National Science Foundation (NSF), Divisions of Chemistry (CHE), and Materials Research (DMR) under grant No. CHE-1834750. Solid-state NMR work at Ames National Laboratory was supported by the U.S. Department of Energy (DOE), Office of Basic Energy Sciences, Division of Chemical Sciences, Geosciences, and Biosciences through a DOE Early Career Project. Ames National Laboratory is operated for the DOE by Iowa State University under Contract No. DE-AC02-07CH11358. T.D.T. thanks the U.S. Department of Energy, Office of Science, Office of Basic Energy Sciences, Chemical Sciences, Geosciences, and Biosciences Division under Contract no. DE-AC02-05CH11231. T.A.G. acknowledges the support of the U.S. DOE, Office of Science, Office of Workforce Development for Teachers and Scientists, Office of Science Graduate Student Research (SCGSR) program. The SCGSR program is administered by the Oak Ridge Institute for Science and Education (ORISE) for the DOE, and ORISE is managed by ORAU under contract No. DE-SC0014664.

Notes

The authors declare no competing financial interest.

REFERENCES

(1) Obligacion, J. V.; Chirik, P. J. Earth-abundant transition metal catalysts for alkene hydrosilylation and hydroboration. *Nat. Rev. Chem.* **2018**, *2* (5), 15−34.

(2) Marciniec, B. Catalysis by transition metal complexes of alkene silylation - recent progress and mechanistic implications. *Coord. Chem. Rev.* **2005**, *249* (21−22), 2374−2390.

(3) Pukhnarevitch, V. B.; Lukevics, E.; Kopylova, L. I.; Voronkov, M. *Perspectives of Hydrosilylation*; Institute for Organic Synthesis: Riga, Latvia, 1992.

(4) Roy, A. K. A Review of Recent Progress in Catalyzed Homogeneous Hydrosilation (Hydrosilylation). In *Advances in Organometallic Chemistry*; Robert West, A. F. H.; Mark, J. F., Eds.; Academic Press, 2007; Vol. *55*, pp 1−59.

(5) Plueddemann, E. *Silane Coupling Agents*, 2nd ed.; Plenum Press: New York, 1991.

(6) Marko, I. E.; Sterin, S.; Buisine, O.; Mignani, G.; Branlard, P.; Tinant, B.; Declercq, J. P. Selective and efficient platinum(0)-carbene complexes as hydrosilylation catalysts. *Science* **2002**, *298* (5591), 204−206.

(7) Buisine, O.; Berthon-Gelloz, G.; Briere, J. F.; Sterin, S.; Mignani, G.; Branlard, P.; Tinant, B.; Declercq, J. P.; Marko, I. E. Second generation N-heterocyclic carbene-Pt(0) complexes as efficient catalysts for the hydrosilylation of alkenes. *Chem. Commun.* **2005**, No. 30, 3856−3858.

(8) Hitchcock, P. B.; Lappert, M. F.; Warhurst, N. J. W. Synthesis and Structure of a Rac-Tris(Divinyldisiloxane)Diplatinum(0) Complex and Its Reaction with Maleic-Anhydride. *Angew. Chem., Int. Ed.* **1991**, *30* (4), 438−440.

(9) Yang, C.-J. An impending platinum crisis and its implications for the future of the automobile. *Energy Policy* **2009**, *37* (5), 1805−1808.

(10) Glaser, P. B.; Tilley, T. D. Catalytic Hydrosilylation of Alkenes by a Ruthenium Silylene Complex. Evidence for a New Hydrosilylation Mechanism. *J. Am. Chem. Soc.* **2003**, *125* (45), 13640−13641.

(11) Calimano, E.; Tilley, T. D. Alkene Hydrosilation by a Cationic Hydrogen-Substituted Iridium Silylene Complex. *J. Am. Chem. Soc.* **2008**, *130* (29), 9226−9227.

(12) Fasulo, M. E.; Lipke, M. C.; Tilley, T. D. Structural and mechanistic investigation of a cationic hydrogen-substituted ruthenium silylene catalyst for alkene hydrosilation. *Chem. Sci.* **2013**, *4* (10), 3882−3887.

(13) Smith, P. W.; Dong, Y.; Tilley, T. D. Efficient and selective alkene hydrosilation promoted by weak, double Si−H activation at an iron center. *Chem. Sci.* **2020**, *11* (27), 7070−7075.

(14) Brunner, H. A New Hydrosilylation Mechanism—New Preparative Opportunities. *Angew. Chem., Int. Ed.* **2004**, *43* (21), 2749−2750.

(15) Beddie, C.; Hall, M. B. A Theoretical Investigation of Ruthenium-Catalyzed Alkene Hydrosilation: Evidence To Support an Exciting New Mechanistic Proposal. *J. Am. Chem. Soc.* **2004**, *126* (42), 13564−13565.

(16) Beddie, C.; Hall, M. B. Do B3LYP and CCSD(T) Predict Different Hydrosilylation Mechanisms? Influences of Theoretical Methods and Basis Sets on Relative Energies in Ruthenium−Silylene-Catalyzed Ethylene Hydrosilylation. *J. Phys. Chem. A* **2006**, *110* (4), 1416−1425.

(17) Böhme, U. Hydrosilylation vs. [2 + 2]-cycloaddition: A theoretical study with iron and ruthenium complexes. *J. Organomet. Chem.* **2006**, *691* (21), 4400−4410.

(18) Tuttle, T.; Wang, D.; Thiel, W.; Köhler, J.; Hofmann, M.; Weis, J. Mechanism of olefin hydrosilylation catalyzed by $[RuCl(NCCH_3)_5]^+$: A DFT study. *J. Organomet. Chem.* **2007**, *692* (11), 2282−2290.

(19) Somerville, R. J.; Campos, J. Cooperativity in Transition Metal Tetrylene Complexes. *Eur. J. Inorg. Chem.* **2021**, *2021* (34), 3488−3498.

(20) Zhang, X.-H.; Chung, L. W.; Lin, Z.; Wu, Y.-D. A DFT Study on the Mechanism of Hydrosilylation of Unsaturated Compounds with Neutral Hydrido(hydrosilylene)tungsten Complex. *J. Org. Chem.* **2008**, *73* (3), 820−829.

(21) Rankin, M. A.; MacLean, D. F.; Schatte, G.; McDonald, R.; Stradiotto, M. Silylene Extrusion from Organosilanes via Double Geminal Si−H Bond Activation by a $Cp^*Ru(\kappa^2\text{-}P,N)^+$ Complex: Observation of a Key Stoichiometric Step in the Glaser−Tilley Alkene Hydrosilylation Mechanism. *J. Am. Chem. Soc.* **2007**, *129* (51), 15855−15864.

(22) Grumbine, S. K.; Mitchell, G. P.; Straus, D. A.; Tilley, T. D.; Rheingold, A. L. Synthesis and Study of Ruthenium Silylene Complexes of the Type $[(\eta^5\text{-}C_5Me_5)(Me_3P)_2RuSiX_2]^+$ (X = Thiolate, Me, and Ph). *Organometallics* **1998**, *17* (26), 5607−5619.

(23) Rufh, S. A.; Goudreault, A. Y.; Foscato, M.; Jensen, V. R.; Fogg, D. E. Rapid Decomposition of Olefin Metathesis Catalysts by a Truncated N-Heterocyclic Carbene: Efficient Catalyst Quenching and N-Heterocyclic Carbene Vinylation. *ACS Catal.* **2018**, *8* (12), 11822−11826.

(24) Joslin, E. E.; McKeown, B. A.; Cundari, T. R.; Gunnoe, T. B. Studies of the decomposition of the ethylene hydrophenylation catalyst TpRu(CO)(NCMe)Ph. *J. Organomet. Chem.* **2017**, *847*, 289−293.

(25) Witzke, R. J.; Chapovetsky, A.; Conley, M. P.; Kaphan, D. M.; Delferro, M. Nontraditional Catalyst Supports in Surface Organometallic Chemistry. *ACS Catal.* **2020**, *10* (20), 11822−11840.

(26) Syed, Z. H.; Kaphan, D. M.; Perras, F. A.; Pruski, M.; Ferrandon, M. S.; Wegener, E. C.; Celik, G.; Wen, J.; Liu, C.; Dogan, F.; Goldberg, K. I.; Delferro, M. Electrophilic Organoiridium(III) Pincer Complexes on Sulfated Zirconia for Hydrocarbon Activation and Functionalization. *J. Am. Chem. Soc.* **2019**, *141* (15), 6325−6337.

(27) Stalzer, M. M.; Delferro, M.; Marks, T. J. Supported Single-Site Organometallic Catalysts for the Synthesis of High-Performance Polyolefins. *Catal. Lett.* **2015**, *145* (1), 3−14.

(28) Klet, R. C.; Kaphan, D. M.; Liu, C.; Yang, C.; Kropf, A. J.; Perras, F. A.; Pruski, M.; Hock, A. S.; Delferro, M. Evidence for Redox Mechanisms in Organometallic Chemisorption and Reactivity on Sulfated Metal Oxides. *J. Am. Chem. Soc.* **2018**, *140* (20), 6308−6316.

(29) Gu, W.; Stalzer, M. M.; Nicholas, C. P.; Bhattacharyya, A.; Motta, A.; Gallagher, J. R.; Zhang, G.; Miller, J. T.; Kobayashi, T.; Pruski, M.; Delferro, M.; Marks, T. J. Benzene Selectivity in Competitive Arene Hydrogenation: Effects of Single-Site Catalyst··· Acidic Oxide Surface Binding Geometry. *J. Am. Chem. Soc.* **2015**, *137* (21), 6770−6780.

(30) Rodriguez, J.; Conley, M. P. Ethylene Polymerization Activity of $(R_3P)Ni(codH)^+$ (cod = 1,5-cylcooctadiene) Sites Supported on Sulfated Zirconium Oxide. *Inorg. Chem.* **2021**, *60* (10), 6946−6949.

(31) Ahn, H.; Nicholas, C. P.; Marks, T. J. Surface Organozirconium Electrophiles Activated by Chemisorption on "Super Acidic" Sulfated Zirconia as Hydrogenation and Polymerization Catalysts. A Synthetic, Structural, and Mechanistic Catalytic Study. *Organometallics* **2002**, *21* (9), 1788−1806.

(32) Zhang, J.; Motta, A.; Gao, Y.; Stalzer, M. M.; Delferro, M.; Liu, B.; Lohr, T. L.; Marks, T. J. Cationic Pyridylamido Adsorbate on Brønsted Acidic Sulfated Zirconia: A Molecular Supported Organohafnium Catalyst for Olefin Homo- and Co-Polymerization. *ACS Catal.* **2018**, *8* (6), 4893−4901.

(33) Stalzer, M. M.; Nicholas, C. P.; Bhattacharyya, A.; Motta, A.; Delferro, M.; Marks, T. J. Single-Face/All-cis Arene Hydrogenation by a Supported Single-Site d^0 Organozirconium Catalyst. *Angew. Chem., Int. Ed.* **2016**, *55* (17), 5263−5267.

(34) Nicholas, C. P.; Ahn, H.; Marks, T. J. Synthesis, Spectroscopy, and Catalytic Properties of Cationic Organozirconium Adsorbates on "Super Acidic" Sulfated Alumina. "Single-Site" Heterogeneous Catalysts with Virtually 100 Active Sites. *J. Am. Chem. Soc.* **2003**, *125* (14), 4325−4331.

(35) Williams, L. A.; Guo, N.; Motta, A.; Delferro, M.; Fragalà, I. L.; Miller, J. T.; Marks, T. J. Surface structural-chemical characterization of a single-site d^0 heterogeneous arene hydrogenation catalyst having 100% active sites. *Proc. Natl. Acad. Sci. U.S.A.* **2013**, *110* (2), 413−418.

https://doi.org/10.1021/acscatal.3c03399
ACS Catal. 2023, 13, 13383−13394

(36) Chen, L.; Ali, I. S.; Sterbinsky, G. E.; Gamler, J. T. L.; Skrabalak, S. E.; Tait, S. L. Alkene Hydrosilylation on Oxide-Supported Pt-Ligand Single-Site Catalysts. *ChemCatChem* **2019**, *11* (12), 2843−2854.
(37) Taccardi, N.; Fekete, M.; Berger, M. E.; Stanjek, V.; Schulz, P. S.; Wasserscheid, P. Catalyst recycling in monophasic Pt-catalyzed hydrosilylation reactions using ionic liquids. *Appl. Catal., A* **2011**, *399* (1), 69−74.
(38) Chauhan, B. P. S.; Sarkar, A. Functionalized vinylsilanes via highly efficient and recyclable Pt-nanoparticle catalysed hydrosilylation of alkynes. *Dalton Trans.* **2017**, *46* (27), 8709−8715.
(39) Zhao, J.; Gui, Y.; Liu, Y.; Wang, G.; Zhang, H.; Sun, Ya.; Fang, S. Highly Efficient and Magnetically Recyclable Pt Catalysts for Hydrosilylation Reactions. *Catal. Lett.* **2017**, *147* (5), 1127−1132.
(40) Fernández, G.; Pleixats, R. Soluble Pt Nanoparticles Stabilized by a Tris-imidazolium Tetrafluoroborate as Efficient and Recyclable Catalyst for the Stereoselective Hydrosilylation of Alkynes. *ChemistrySelect* **2018**, *3* (41), 11486−11493.
(41) Jawale, D. V.; Geertsen, V.; Miserque, F.; Berthault, P.; Gravel, E.; Doris, E. Solvent-free hydrosilylation of alkenes and alkynes using recyclable platinum on carbon nanotubes. *Green Chem.* **2021**, *23* (2), 815−820.
(42) Van Do, D.; Hosokawa, T.; Horiuchi, Y.; Matsuoka, M. Carbon-coated mesoporous silica incorporating organoruthenium complexes and its application to hydrosilylation of 1-hexyne. *Res. Chem. Intermed.* **2020**, *46* (12), 5297−5306.
(43) Seçkin, T. K.; Süleyman; Özdemir, İ.; Çetinkaya, B. Synthesis of a Ruthenium Complex Bound to a Polyimide Matrix: Investigating the Catalytic Properties in a Hydrosilylation Reaction. *Turk. J. Chem.* **2006**, *30* (1), 93−101.
(44) Li, M.; Zhao, S.; Li, J.; Chen, X.; Ji, Y.; Yu, H.; Bai, D.; Xu, G.; Zhong, Z.; Su, F. Partially charged single-atom Ru supported on ZrO_2 nanocrystals for highly efficient ethylene hydrosilylation with triethoxysilane. *Nano Res.* **2022**, *15* (7), 5857−5864.
(45) Arliguie, T.; Border, C.; Chaudret, B.; Devillers, J.; Poilblanc, R. Chloro- and hydrido(pentamethylcyclopentadienyl)ruthenium complexes: anomalous NMR behavior of $C_5Me_5RuH_3PR_3$ (R = $CHMe_2$, Cy). *Organometallics* **1989**, *8* (5), 1308−1314.
(46) Wakatsuki, Y.; Yamazaki, H. Some organometallic chemistry of ruthenium(II). *J. Organomet. Chem.* **1995**, *500* (1), 349−362.
(47) Hayes, P. G.; Waterman, R.; Glaser, P. B.; Tilley, T. D. Synthesis, Structure, and Reactivity of Neutral Hydrogen-Substituted Ruthenium Silylene and Germylene Complexes. *Organometallics* **2009**, *28* (17), 5082−5089.
(48) Haw, J. F.; Zhang, J.; Shimizu, K.; Venkatraman, T. N.; Luigi, D.-P.; Song, W.; Barich, D. H.; Nicholas, J. B. NMR and Theoretical Study of Acidity Probes on Sulfated Zirconia Catalysts. *J. Am. Chem. Soc.* **2000**, *122* (50), 12561−12570.
(49) Rodriguez, J.; Culver, D. B.; Conley, M. P. Generation of Phosphonium Sites on Sulfated Zirconium Oxide: Relationship to Brønsted Acid Strength of Surface − OH Sites. *J. Am. Chem. Soc.* **2019**, *141* (4), 1484−1488.
(50) Baltusis, L.; Frye, J. S.; Maciel, G. E. Phosphine oxides as NMR probes for adsorption sites on surfaces. *J. Am. Chem. Soc.* **1986**, *108* (22), 7119−7120.
(51) Dioumaev, V. K.; Procopio, L. J.; Carroll, P. J.; Berry, D. H. Synthesis and Reactivity of Silyl Ruthenium Complexes: The Importance of Trans Effects in C−H Activation, Si−C Bond Formation, and Dehydrogenative Coupling of Silanes. *J. Am. Chem. Soc.* **2003**, *125* (26), 8043−8058.
(52) Smith, E. E.; Du, G.; Fanwick, P. E.; Abu-Omar, M. M. Dehydrocoupling of Organosilanes with a Dinuclear Nickel Hydride Catalyst and Isolation of a Nickel Silyl Complex. *Organometallics* **2010**, *29* (23), 6527−6533.
(53) Rosenberg, L.; Kobus, D. N. Dehydrogenative coupling of primary alkyl silanes using Wilkinson's catalyst. *J. Organomet. Chem.* **2003**, *685* (1), 107−112.
(54) Copéret, C.; Comas-Vives, A.; Conley, M. P.; Estes, D. P.; Fedorov, A.; Mougel, V.; Nagae, H.; Núñez-Zarur, F.; Zhizhko, P. A. Surface Organometallic and Coordination Chemistry toward Single-Site Heterogeneous Catalysts: Strategies, Methods, Structures, and Activities. *Chem. Rev.* **2016**, *116* (2), 323−421.
(55) Gruber, S.; Zaitsev, A. B.; Wörle, M.; Pregosin, P. S.; Veiros, L. F. Rapid, Selective Ru-Sulfonate-Catalyzed Allylation of Indoles Using Alcohols as Substrates. *Organometallics* **2009**, *28* (12), 3437−3448.
(56) Goldslager, B. A.; Clarson, S. J. Dehydrogenative Coupling of Poly(phenylsilane) by Metallocene Catalysis. *J. Inorg. Organomet. Polym.* **1999**, *9* (2), 123−131.
(57) Fasulo, M. E.; Glaser, P. B.; Tilley, T. D. Cp*(^{i}Pr$_3$P)RuOTf: A Reagent for Access to Ruthenium Silylene Complexes. *Organometallics* **2011**, *30* (20), 5524−5531.
(58) Copéret, C.; Estes, D. P.; Larmier, K.; Searles, K. Isolated Surface Hydrides: Formation, Structure, and Reactivity. *Chem. Rev.* **2016**, *116* (15), 8463−8505.
(59) Kaplan, A. W.; Bergman, R. G. Nitrous Oxide Mediated Synthesis of Monomeric Hydroxoruthenium Complexes. Reactivity of $(DMPE)_2Ru(H)(OH)$ and the Synthesis of a Silica-Bound Ruthenium Complex. *Organometallics* **1998**, *17* (23), 5072−5085.
(60) Berthoud, R.; Baudouin, A.; Fenet, B.; Lukens, W.; Pelzer, K.; Basset, J.-M.; Candy, J.-P.; Copéret, C. Mononuclear Ruthenium Hydride Species versus Ruthenium Nanoparticles: The Effect of Silane Functionalities on Silica Surfaces. *Chem. - Eur. J.* **2008**, *14* (12), 3523−3526.
(61) Maly, T.; Debelouchina, G. T.; Bajaj, V. S.; Hu, K.-N.; Joo, C.-G.; Mak−Jurkauskas, M. L.; Sirigiri, J. R.; van der Wel, P. C. A.; Herzfeld, J.; Temkin, R. J.; Griffin, R. G. Dynamic nuclear polarization at high magnetic fields. *J. Chem. Phys.* **2008**, *128* (5), No. 052211.
(62) Lesage, A.; Lelli, M.; Gajan, D.; Caporini, M. A.; Vitzthum, V.; Miéville, P.; Alauzun, J.; Roussey, A.; Thieuleux, C.; Mehdi, A.; Bodenhausen, G.; Coperet, C.; Emsley, L. Surface Enhanced NMR Spectroscopy by Dynamic Nuclear Polarization. *J. Am. Chem. Soc.* **2010**, *132* (44), 15459−15461.
(63) Kobayashi, T.; Perras, F. A.; Slowing, I. I.; Sadow, A. D.; Pruski, M. Dynamic Nuclear Polarization Solid-State NMR in Heterogeneous Catalysis Research. *ACS Catal.* **2015**, *5* (12), 7055−7062.
(64) Feigl, A.; Chiorescu, I.; Deller, K.; Heidsieck, S. U. H.; Buchner, M. R.; Karttunen, V.; Bockholt, A.; Genest, A.; Rösch, N.; Rieger, B. Metal-Free Polymerization of Phenylsilane: Tris(pentafluorophenyl)-borane-Catalyzed Synthesis of Branched Polysilanes at Elevated Temperatures. *Chem. - Eur. J.* **2013**, *19* (37), 12526−12536.
(65) Jutzi, P.; Redeker, T.; Neumann, B.; Stammler, H.-G. Titanium and Zirconium Bent-Sandwich Complexes with the New [2-(Diisopropylamino)ethyl]cyclopentadienyl Ligand: Catalysts for the Polymerization of Ethylene and the Dehydrocoupling of Phenylsilane. *Organometallics* **1996**, *15* (20), 4153−4161.
(66) Woo, H. G.; Tilley, T. D. Dehydrogenative polymerization of silanes to polysilanes by zirconocene and hafnocene catalysts. A new polymerization mechanism. *J. Am. Chem. Soc.* **1989**, *111* (20), 8043−8044.
(67) Culver, D. B.; Conley, M. P. Activation of C−F Bonds by Electrophilic Organosilicon Sites Supported on Sulfated Zirconia. *Angew. Chem., Int. Ed.* **2018**, *57* (45), 14902−14905.
(68) Curtis, M. D.; Epstein, P. S. Redistribution Reactions on Silicon Catalyzed by Transition Metal Complexes. In *Advances in Organometallic Chemistry*; Stone, F. G. A.; West, R., Eds.; Academic Press, 1981; Vol. *19*, pp 213−255.
(69) Choi, N.; Onozawa, S.-Y.; Sakakura, T.; Tanaka, M. Dehydrocoupling of Phenylsilane Catalyzed by (Dimethylamino)-alkyl- or Branched-Alkyl-Substituted Zirconocene Complexes: An Alternative Approach to Longer Chains. *Organometallics* **1997**, *16* (13), 2765−2767.
(70) Said, R. B.; Hussein, K.; Barthelat, J.-C.; Atheaux, I.; Sabo-Etienne, S.; Grellier, M.; Donnadieu, B.; Chaudret, B. Redistribution at silicon by ruthenium complexes. Bonding mode of the bridging silanes in $Ru_2H_4(\mu\text{-}\eta^2{:}\eta^2{:}\eta^2{:}\eta^2\text{-}SiH_4)(PCy_3)_4$ and $Ru_2H_2(\mu\text{-}\eta^2{:}\eta^2\text{-}H_2Si(OMe)_2)_3(PCy_3)_2$. *Dalton Trans.* **2003**, No. 21, 4139−4146.
(71) Bligaard, T.; Bullock, R. M.; Campbell, C. T.; Chen, J. G.; Gates, B. C.; Gorte, R. J.; Jones, C. W.; Jones, W. D.; Kitchin, J. R.;

Scott, S. L. Toward Benchmarking in Catalysis Science: Best Practices, Challenges, and Opportunities. *ACS Catal.* **2016**, *6* (4), 2590−2602.

https://doi.org/10.1021/acscatal.3c03399
ACS Catal. 2023, 13, 13383−13394